DOI: 10.1002/ejic.200900613

Polyoxothiomolybdenum Wheels as Anionic Receptors for Recognition of Sulfate and Sulfonate Anions

Jean-François Lemonnier,[a] Sébastien Floquet,*[a] Jérôme Marrot,[a] and Emmanuel Cadot*[a]

Keywords: Molybdenum / Polyoxometalates / Sulfur / Molecular recognition / Self-assembly

The formation of supramolecular host–guest cyclic architectures, built up through the self-condensation process of $[Mo_2O_2S_2]^{2+}$ oxothiocations driven by sulfate and sulfonate anions is reported. The complexes $[(SO_4)_2Mo_{10}O_{10}S_{10}(OH)_{10}(H_2O)_5]^{4-}$ and $[(EtSO_3)_2Mo_{10}O_{10}S_{10}(OH)_{10}(H_2O)_5]^{2-}$ were characterized in the solid state by X-ray diffraction, and particular attention was given to the analysis of the hydrogen-bonding interactions, which ensure the host–guest stability of such architectures. Taking into account these properties, we report preliminary results on the grafting of oxothiomolybdenum cyclic materials onto sulfonated resin such as Dowex 50–80.

Introduction

Polyoxometalates (POMs) represent a family of inorganic compounds rich of thousands of compounds that are of current interest for recognized applications in catalysis,[1–5] medicine[6,7] magnetism,[8,9] or in supramolecular chemistry.[10–14] In marked contrast with POMs, polyoxothiometalates (POTMs) are far less common, but they can provide original compounds and especially transition-metal-ring-like clusters based on the self-condensation of $[M_2O_2S_2]^{2+}$ oxothiocations (M = Mo^V or W^V).[15] In contrast to the standard structures of polyoxometalates, these compounds are characterized by a host–guest self-adaptability. The self-assembly process can be controlled by templating agents, mainly anionic groups such as phosphates[16,17] metalates,[18] or polycarboxylates,[19–23] which are encapsulated covalently as guests in the adapted central cavity. In the presence of halides, supramolecular assemblies based on hydrogen bonding with water molecules within the cavity of the ring were evidenced in the solid state and in solution, thus highlighting anionic recognition properties for this class of compounds.[24,25] We notably established that supramolecular interactions between inner water molecules and halides in solution increase in the following sequence $I^- < Br^- < Cl^-$.[16] In this context, we were interested to extend this study to the interactions of molybdenum rings with sulfates and sulfonates by keeping in mind the possible extension of this work for the preparation of polymeric materials incorporating molybdenum rings. Herein, we report the synthesis and the characterization of two new decamolybdenum rings self-assembled around sulfate or ethylsulfonate anions. Such host–guest interactions open the way for immobilization of these cyclic compounds by functionalized surfaces, such as sulfonated resins.

[a] Institut Lavoisier de Versailles, UMR 8180, University of Versailles,
45 avenue des Etats-Unis, 78035 Versailles, France
E-mail: sebastien.floquet@chimie.uvsq.fr
cadot@chimie.uvsq.fr

Results

Syntheses

Some years ago, we demonstrated that the condensation of $[Mo_2O_2S_2]^{2+}$ oxothiocations in aqueous media in the presence of halides led to $[X_2Mo_{10}O_{10}S_{10}(OH)_{10}(H_2O)_5]^{2-}$ systems where a decamolybdenum ring is bicapped by two halide ions through a convergent hydrogen-bonding network. Furthermore, in nearly pure water, at pH 3, the halide-containing decamolybdenum rings evolve towards the formation of the neutral dodecamolybdenum ring $[Mo_{12}O_{12}S_{12}(OH)_{12}(H_2O)_6]$.[26] At pH values above 5, the inner water molecules of the Mo rings are deprotonated successively to give anionic compounds such as $[Mo_{10}O_{10}S_{10}(OH)_{12}(H_2O)_3]^{2-}$ or $[Mo_8O_8S_8(OH)_{10}(H_2O)]^{2-}$. Such acid–base processes change the ionic character of the inner cavity from cationic to anionic. Consequently, the synthesis of sulfate or sulfonate-containing rings presented in this study were carried out below pH 5 to keep the inner cavity cationic.[24–27] Under these conditions, the self-assembly of the $[Mo_2O_2S_2]^{2+}$ oxothiocations in the presence of an excess amount of sulfate or ethylsulfonate anions gives the exclusive complexes $[(SO_4)_2Mo_{10}O_{10}S_{10}(OH)_{10}(H_2O)_5]^{4-}$ {**1**; $[(SO_4)_2Mo_{10}]^{4-}$} and $[(EtSO_3)_2Mo_{10}O_{10}S_{10}(OH)_{10}(H_2O)_5]^{2-}$ {**2**; $[(EtSO_3)_2Mo_{10}]^{2-}$}, which were isolated in moderate yield.

Structures of the Anions

The molecular structures of decamolybdenum rings self assembled by sulfate and ethylsulfonate anions are shown in Figures 1–4, whereas crystal data are given in Table 2. A basic description of the molecular architectures consists of two host anions interacting closely with a cyclic inorganic neutral skeleton $[Mo_{10}S_{10}O_{10}(OH)_{10}(H_2O)_5]$, which appears very similar in both molecular arrangements **1** and **2** (Figure 1). Five $\{Mo_2S_2O_2\}$ building blocks are connected through double hydroxido bridging ligands {Mo–O distances in the range [2.067(2)–2.131(2) Å]} and five bridging water molecules {Mo–O distances in the range [2.483(2) to 2.615(2) Å]}, which span nonbonding Mo–Mo contacts [3.299(2)–3.341(2) Å] alternating with short Mo–Mo bonding contacts within the building blocks [2.836(2)–2.866(2) Å]. Interestingly, both structures strongly differ from the compound reported by Kabanos and co-workers with sulfite anions.[28] In this case, probably due to a higher basicity of the sulfites compared to sulfates and sulfonates, the sulfites are coordinated to the $[Mo_2O_2S_2]^{2+}$ cations to give a spectacular cluster including 6 oxothiocations and 16 bridging sulfites ligands.

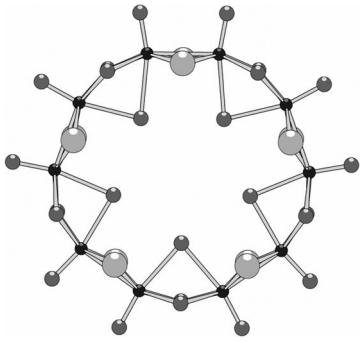

Figure 1. Structural representation of the inorganic cyclic host present in **1** and **2** (color code: medium grey spheres O, small black spheres Mo, large light grey spheres S).

$[2SO_4^{2-}\subset\{Mo_{10}O_{10}S_{10}(OH)_{10}(H_2O)_5\}]$ (1)

The molecular structure of the $[(SO_4)_2Mo_{10}]^{4-}$ anion is depicted in Figure 2. X-ray diffraction analysis revealed that two independent $[(SO_4)_2Mo_{10}]^{4-}$ molecular units are present in the cell. One retains no symmetry in the solid state, whereas the other exhibits a C_2 axis contained in the averaged plan defined by the Mo atoms. Therefore, both units exhibit close arrangements with similar geometrical parameters, and for clarity, averaged geometrical parameters will be used for the structural description. The presence of two sulfate anions on both sides of the ring is a striking feature of the structure. The two sulfate anions are almost symmetrically located on both sides of the Mo ring but adopt an eclipsed relative arrangement. The supramolecular host–guest arrangement is derived from those previously reported with I^- or Cl^- ions[24,25] and involves the five inner polarized water molecules. The two sulfates are put on the five inner water molecules, like tripodal groups. The three oxygen atoms of both $\{SO_3\}$ tripods interact with the five inner water molecules through a convergent hydrogen-bonding network. One oxygen atom (labeled Os) belonging to the $\{SO_3\}$ tripod is singly hydrogen bonded to one aqua ligand and exhibits a short S–Os bond [1.31(2) Å]. The other two oxygen atoms (labeled Ob) bridge a pair of adjacent water molecules and give longer S–Ob bond lengths [1.42(2) Å]. The fourth oxygen atom labeled Ot points to outer the cavity through a long S–Ot bond length [1.37(2) Å]. The presence of three long S–O bonds and a single shorter one gives an approximate C_{3v} local symmetry, consistent with the infrared data (see below). Furthermore, the distribution of the four S–O bonds distances reflects the hydrogen-bonding pathway within the host–guest system. Each Ob atom that interact with two adjacent water molecules gives two close O···O contacts (2.67 and 2.80 Å). The third S–Os bond give a single hydrogen-bond interaction with an O···O contact of about 2.80 Å. Interestingly, the terminal {S–Ot} group exhibits a long bond lengths [1.37(2) Å] for such a situation. Actually, the Ot oxygen atom interacts through hydrogen bonds with two uncoordinated water molecules, giving the shortest O···O contacts (2.57 and 2.59 Å, Figure 3). The averaged bond lengths involving the sulfate groups in **1** are summa-

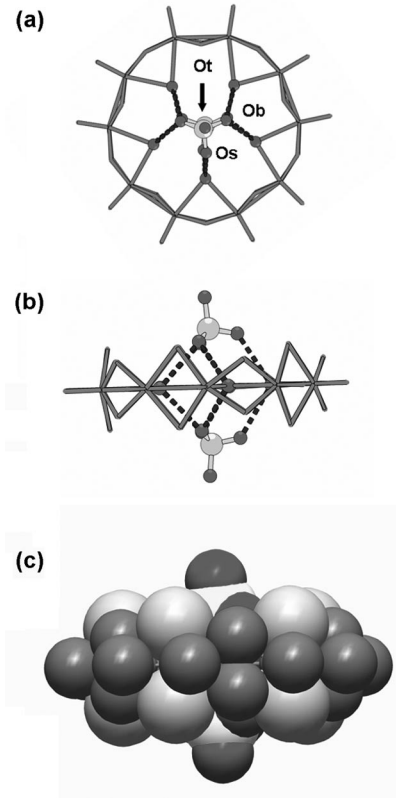

Figure 2. Molecular representations of **1**: (a) top and side view highlighting the host–guest interactions between sulfate groups (ball-and-stick representation) and the inorganic ring (grey-stick representation). The labeled oxygen atoms of the $\{SO_4\}$ group, the bridging hydrogen bond, the single hydrogen bond, and the terminal oxygen atoms are labeled Ob, Os, and Ot, respectively; (b) space-filling representation showing the embedded sulfate groups within the $\{Mo_{10}\}$ ring.

rized in Table 1. Furthermore, The $\{SO_3\}$ tripod of each sulfate group appears significantly tilted at about 20° with respect to the averaged plane defined by the 10 Mo atoms of the cycle, probably due to the complex surrounding hydrogen-bond distributions. An examination of the packing reveals a nice 2D network built upon hydrogen-bond connections involving the {S–Ot} groups and uncoordinated water molecules. Three host–guest units $[2SO_4^{2-}\subset\{Mo_{10}\}]$ are arranged around two crystallization water molecules through the strongest hydrogen bonds involving the {S–Ot} groups, leading to a C_3 idealized assembly (see Figure 3a). Finally, both opposite sulfate groups within the $\{Mo_{10}\}$ rings act as ditopic hydrogen-bond connectors able to produce the polymeric 2D anionic network through hydrogen-bond connections in the *ab* plane (see Figure 3b).

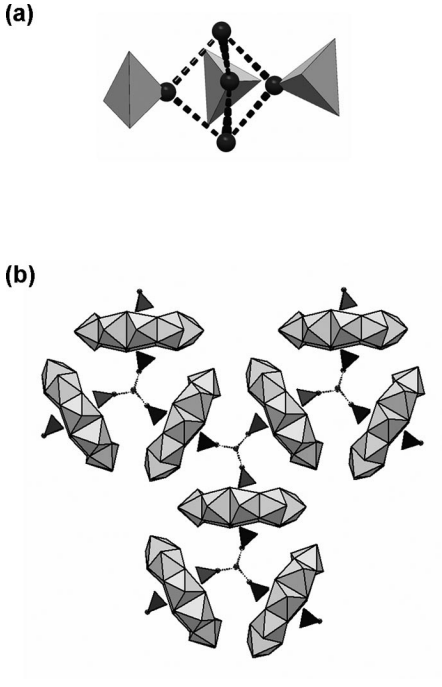

Figure 3. (a) Representation of the outer hydrogen-bonding interactions between the three sulfate groups and two water molecules; (b) the $[2SO_4^{2-}\subset\{Mo_{10}\}]$ building blocks act as ditopic connectors able to produce a 2D hydrogen-bonding network in the *ab* plane.

Table 1. Selected averaged bond lengths in **1**.

S–Os	1.31(4)	Os···O	2.80(10)
S–Ob	1.42(2)	Ob···O	2.67(8)
S–Ot	1.37(5)		2.80(8)
		Ot···O	2.57(10)
			2.59(10)

[2(EtSO$_3$)⊂{Mo$_{10}$O$_{10}$S$_{10}$(OH)$_{10}$(H$_2$O)$_5$}] (2)

The structure of **2** (Figure 4) consists of a neutral molybdenum ring $[Mo_{10}S_{10}O_{10}(OH)_{10}(H_2O)_5]$ associated with two ethylsulfonate anions $EtSO_3^-$. The host–guest interaction appears rather similar to those observed in the structure of $[(2SO_4^{2-})\subset\{Mo_{10}\}]^{4-}$ (**1**) described above. Both ethylsulfonate anions are positioned on both sides of the molybdenum ring where the $\{SO_3\}$ tripods interact with the five inner water molecules through hydrogen bonds. However, the resulting hydrogen-bonding network differs slightly from that observed in **1**. Using the same terminology for the structural description of **1**, both $\{SO_3\}$ units in **2** contain one Ob-type and two Os-type oxygen atoms. All the S–O distances appears nearly similar and fall in the 1.41(1)–1.45(1) Å range. The hydrogen-bond-bridging Ob atoms are engaged in two nearly O···O contacts with two adjacent aqua ligand (2.65 Å), whereas the Os atoms are singly hydrogen bonded through a significantly longer O···O contact (2.78 Å). One $\{SO_3\}$ tripod appears equally disordered over two equivalent positions created by a mirror plane. The Ob oxygen atoms of the two opposite $\{SO_3\}$ groups appear staggered of about 144°. As already observed for **1**, the $\{SO_3\}$ tripods are also tilted from the averaged plane of the Mo atoms by about 20–25°.

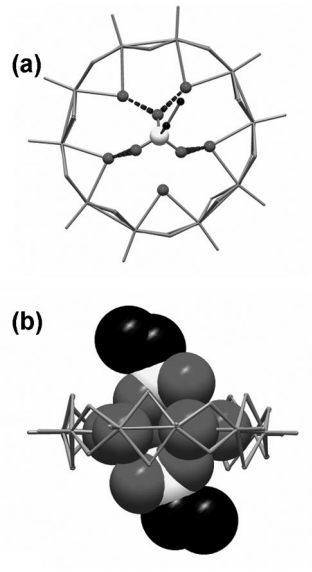

Figure 4. Molecular representation of **2**: (a) the hydrogen-bonding network between the $\{SO_3\}$ tripod of the ethylsulfonate ion and the five inner water molecules of the inorganic ring (grey stick); (b) mixed stick- and space-filling representation showing the close interaction between the ethylsulfonate and the five inner water molecules.

FTIR Spectra

The FTIR spectra of compounds **1** and **2** are depicted in Figure 5. For both compounds, the strong absorptions observed near 970 and 520 cm^{-1} correspond to the fingerprint of the inorganic oxothiomolybdenum wheels. The former is assigned to Mo=O stretching modes, whereas the latter is assigned to the breathing mode of the Mo–(μ-E)$_2$–Mo cyclic skeleton (E = S or OH).[29] The presence of sulfate ions in **1** is observed as two absorption bands at 1134 and 1108 cm^{-1} (Figure 5a), corresponding to the ν_{as}(S–O) stretching modes. Such a feature indicates an approached C_{3v} symmetry for both sulfate groups within **1**, giving the two vibration modes A_1 and E. This result is consistent with the host–guest structure where the two sulfate groups inter-

act with the five inner water molecules through a SO_3 tripod. Such interactions provide three long S–O bonds (≈1.40 Å) and one shorter (≈1.30 Å), in agreement with the IR pattern of the {SO_4} groups.

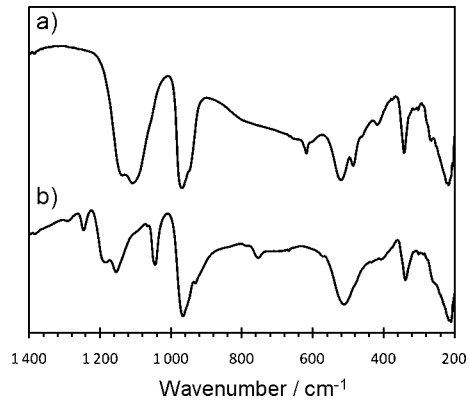

Figure 5. FTIR spectra of (a) **1** and (b) **2**.

The IR spectra of **2** (Figure 5b) consists of three bands at 1183, 1155, and 1045 cm^{-1} related to the presence of the ethylsulfonate anions and two strong absorptions at 970 and 510 cm^{-1}, characteristic of the decamolybdenum ring. The high frequency absorptions at 1183 and 1155 cm^{-1} are assigned to the antisymmetric stretching modes A_1 + E of the sulfonate group, whereas the 1045 cm^{-1} absorption corresponds to the symmetric A_1 mode. These features are typical of the {SO_3C} moiety.

Study in Solution

The behavior of ethylsulfonate-containing compounds **2** was studied in aqueous solution by ^1H NMR (1D and DOSY experiments) spectroscopy with the aim to evidence the host–guest interactions. The ^1H NMR spectrum of **2** displays the signals of the ethylsulfonate ion observed as a triplet at δ = 1.16 ppm (3 H) and a quadruplet at δ = 2.79 ppm (2 H). In the same concentration ranges, $NaEtSO_3$ solutions [(Mo_{10})-free solution] give an ^1H NMR spectrum that is identical with that obtained from **2**. Besides, DOSY experiments were carried out on solutions of **2** and $NaEtSO_3$. Equal values for the self-diffusion coefficient of $EtSO_3^-$ were found, which is fully consistent with an uncoordinated $EtSO_3^-$ ion. These results show that the host–guest system is labile and dissociates in aqueous solution.

Immobilization of the {Mo_{10}} Ring on Sulfonated Resin

The structural polymeric backbone of Dowex-type ion exchangers is constituted of styrene cross-linked with divinyl benzene functionalized with sulfonic acid groups.[30] In this context, hydrogen-bond interactions between inorganic rings and sulfonate functions grafted on resins can be expected, thus constituting a way towards the immobilization of such cyclic materials on a surface. Such a purpose represents a key step for the use of these compounds in catalysis and/or electrocatalysis.

The sorption processes of the neutral compound $[Mo_{10}O_{10}S_{10}(OH)_{10}(H_2O)_5]$ were studied in water at pH 3.5 by UV/Vis spectroscopy.[31] The batch method was used by mixing a constant quantity of dry resin in the sodium form (100 mg) with a variable quantity of $K_2[I_2Mo_{10}O_{10}S_{10}(OH)_{10}(H_2O)_5]$ ranging from 0 to 1.5×10^{-3} M. The resulting suspensions were stirred for 2 h and then left to stand overnight. The resulting filtrates were then analyzed by UV/Vis spectroscopy in comparison with blank experiments without resin. Figure 6 displays the variations of the [Mo_{10}] concentrations of the resulting solutions without and after contact with resin as a function of the introduced [Mo_{10}] concentrations. As expected, without resin, the experimental curve agrees with a Beer–Lambert law in the $0–1.5\times10^{-3}$ M concentration range. Interestingly, the variations in the [Mo_{10}] concentrations after contact with resin is linear with a weaker slope, which demonstrate that adsorption of $[Mo_{10}O_{10}S_{10}(OH)_{10}(H_2O)_5]$ occurs on the resin. As the yellow color of the solution decreases, the color of the resin changes from light-brown to yellowish. The quantity of adsorbed Mo ring can be calculated by the difference between the two curves, which allows a partition number P of the $[Mo_{10}O_{10}S_{10}(OH)_{10}(H_2O)_5]$ with $P = [Mo_{10}]_{adsorbed}/[Mo_{10}]_{free}$ to be calculated. The partition number was found to be constant and equal to 0.85 whatever the quantity of $[Mo_{10}O_{10}S_{10}(OH)_{10}(H_2O)_5]$ added, which correspond to an adsorption of ca. 46–48% of the $[Mo_{10}O_{10}S_{10}(OH)_{10}(H_2O)_5]$ initially introduced into solution. The EDX analysis of washed samples of the resin isolated after contact with a millimolar solution of $[Mo_{10}O_{10}S_{10}(OH)_{10}(H_2O)_5]$ shows only the presence of S, Mo, Na, and K atoms in the sample. The presence of Mo ring on the resin is thus confirmed. Nevertheless, the atomic ratio S/Mo given by the EDX analysis provides an estimate of the Mo rings per available sulfonate group (noted S_{res}). A ratio S_{res}/Mo_{10} of about 200 was found, which indicates a low Mo_{10} loading

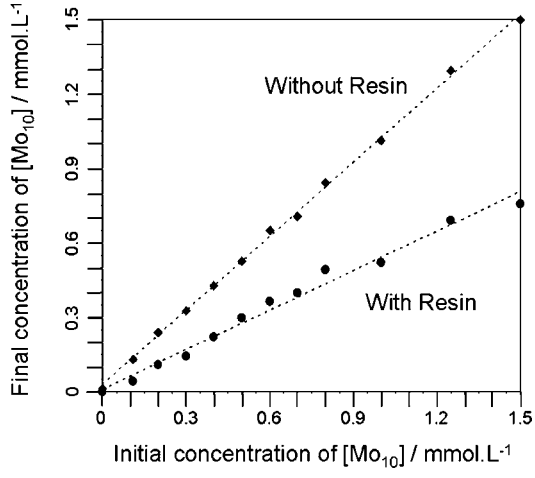

Figure 6. Variation of the [Mo_{10}] concentration without and after contact with dry resin (100 mg, sodium form) at pH 3.5.

on the resin. Finally, similar experiments were carried out with the sulfate-containing ring $[2(SO_4^{2-})\subset\{Mo_{10}\}]$ (**1**). The results reveal a lower $\{Mo_{10}\}$ loading of about 15%, thus suggesting competitive interactions between the sulfonate group of the resin and the sulfate ions in solution. The sorption process should be also dependent upon the nature of the cations. The latter could be also invoked in competitive processes in the vicinity of the grafted sulfonate groups.

Conclusions

In the present study, we show that Mo rings behave as anionic receptors towards sulfate and sulfonate anions. Two compounds were isolated and characterized in the solid state by X-ray diffraction, infrared spectroscopy, and elemental analysis. Both are based on a decamolybdenum ring that contains either two sulfate or two ethylsulfonate ions closely embedded in the center of the cavity. As preliminary results, we present how the $[Mo_{10}]$ ring can be loaded on sulfonated resins. The supramolecular interactions, through a hydrogen-bonding network between grafted sulfonates and the neutral ring, should be at the origin of the immobilization process. We plan to extend this work to other functionalized surfaces.

Experimental Section

Physical Methods: The water content was determined by thermal gravimetric analysis (tga7, Perkin–Elmer). Infrared spectra were recorded with a Magna 550 Nicolet spectrophotometer using KBr pellets. NMR measurements were performed with a Bruker Avance 300 operating at 300 MHz in 5-mm tubes. Chemical shifts were referenced to the external TMS standard. UV/Vis spectra were recorded with a Perkin–Elmer Lambda 19 spectrophotometer in 1 mm quartz cells. Elemental analyses were performed by the Service Central d'Analyses Elémentaires du CNRS, 69390 Vernaison, France. EDX measurements were carried out with a JEOL JSM 5800LV apparatus.

X-ray Crystallography: Single crystals of $K_{3.67}(NMe_4)_{0.33}[(SO_4)_2Mo_{10}O_{10}S_{10}(OH)_{10}(H_2O)_5]\cdot 11H_2O$ and $Rb(NMe_4)[(EtSO_3)_2Mo_{10}O_{10}S_{10}(OH)_{10}(H_2O)_5]\cdot 7H_2O$ (**1** and **2**, respectively) are air sensitive and were recorded in capillaries at 293 K. X-ray intensity data were collected with a Bruker-Nonius X8-APEX2 CCD area-detector diffractometer by using Mo-K_α radiation (λ = 0.71073 Å). Data reduction was accomplished using SAINT V7.03 (APEX2 version 1.0–8; Bruker AXS: Madison, WI, 2003). The substantial redundancy in data allowed a semiempirical absorption correction (SADABS V2.10) to be applied on the basis of multiple measurements of equivalent reflections. The structures were solved by direct methods, developed by successive difference Fourier syntheses, and refined by full-matrix least-squares on all F_2 data using SHELXTL V6.12 (SHELXTL version 6.12; Bruker AXS: Madison, WI, 2001). The dimensions of the crystals and crystallographic data are reported in Table 2. For both complexes, hydrogen atoms of the NMe_4^+ or $EtSO_3^-$ ions were included in calculated positions and allowed to ride on their parent atoms. In the case of **1** we can note that the potassium cations are found disordered with the lattice water molecules. Moreover the O–O distances in the crystal cell did not evidence the presence of Na^+ cations, which are usually characterized by distances from water molecules of about 2.3 Å. Concerning **2**, a mirror plan was found perpendicular to the plane defined by the 10 molybdenum atoms. At first, $EtSO_3^-$ is organized symmetrically to this mirror plan, except for the C2 atom, which is delocalized over two equivalent positions (SOF = 0.5). For the second $EtSO_3^-$ anion, the ethyl group and the central sulfur atom are found on the mirror plan but the three oxygen atoms of the sulfonate group are each disordered on two equivalent positions (SOF = 0.5). Finally, for both compounds, it is worth noting that the discrepancies concerning the amount of hydration water molecules between formulae determined by elemental analyses and X-ray structure is due to difficulty in locating confidently the latter in the crystals due to their number and their high disorder in the solid-state structure. CCDC-738016 (for **2**) and -738017 (for **1**) contain the supplementary crystallographic data for this paper. These data can be obtained free of charge from the Cambridge Crystallographic Data Centre via www.ccdc.cam.ac.uk/data_request/cif.

Table 2. Structural parameters for $K_{3.67}(NMe_4)_{0.33}[(SO_4)_2Mo_{10}]\cdot 11H_2O$ (**1**) and $Rb(NMe_4)[(EtSO_3)_2Mo_{10}]\cdot 7H_2O$ (**2**).

Compound	**1**	**2**
Empirical formula	$C_{1.33}H_{46}K_{3.67}Mo_{10}N_{0.33}O_{44}S_{12}$	$C_8H_{56}Mo_{10}NO_{38}RbS_{12}$
Formula weight	2238.38	2204.13
Temperature / K	293(2)	293(2)
Crystal size / mm	$0.18\times0.10\times0.04$	$0.24\times0.18\times0.18$
Crystal system	monoclinic	orthorhombic
space group	*C*2/*c*	*Pnma*
a / Å	34.495(9)	19.5907(10)
b / Å	19.848(5)	15.9154(10)
c / Å	31.167(10)	18.0753(13)
α / °	90	90
β / °	102.314(8)	90
γ / °	90	90
V / Å^3	20848(10)	5635.8(6)
Z	12	4
$D_{calcd.}$ /g cm^{-3}	2.139	2.598
μ / mm^{-1}	2.400	3.539
F(000)	12840	4256
Data/restraints/parameters	18307/3/1055	8187/7/357
R_{int}	0.1341	0.0542
Final *R* indices [$I>2\sigma(I)$]	R_1 = 0.0951, wR_2 = 0.2537	R_1 = 0.0459, wR_2 = 0.1365

Syntheses: The precursor $K_{2-x}(NMe_4)_x[I_2Mo_{10}O_{10}S_{10}(OH)_{10}(H_2O)_5]\cdot 20H_2O$ ($0 < x < 0.5$) was prepared as described previously in the literature[25] and checked by routine methods. All solvents and reagents were purchased from Aldrich or Acros Chemicals.

$Na_{0.67}(NMe_4)_{0.33}K_3[(SO_4)_2Mo_{10}O_{10}S_{10}(OH)_{10}(H_2O)_5]\cdot 14H_2O$ (1): To a suspension of the precursor $K_{2-x}(NMe_4)_x[I_2Mo_{10}O_{10}S_{10}(OH)_{10}(H_2O)_5]\cdot 20H_2O$ (1 g, ca. 0.42 mmol) in water (20 mL) was added concentrated sulfuric acid (1 mL). The resulting red solution was centrifuged to remove some insoluble yellow precipitate, and the pH of the filtrate was adjusted to 3.5 with aqueous KOH (4 M). A yellow precipitate corresponding to the crude product $(NMe_4)_xK_{3-x}[(SO_4)_2Mo_{10}O_{10}S_{10}(OH)_{10}(H_2O)_5]\cdot xH_2O$ was formed and isolated by filtration, washed by ethanol and ether, and dried in air (0.57 g, 57%). This crude product was recrystallized from aqueous NaCl solution (typically 100 mg in 10 mL). After evaporation of the solvent in air for a few days, yellow hexagonal plates were obtained (0.26 g, 45%), which were isolated by filtration, washed with cold water, and dried in air. IR (KBr): $\tilde{\nu}$ = 1484 (w, NMe_4^+), 1138 (sh., SO_4^{2-}), 1105 (s, SO_4^{2-}), 968 (s), 520 (s), 486 (m) cm^{-1}. $Na_{0.67}(NMe_4)_{0.33}K_3[(SO_4)_2Mo_{10}O_{10}S_{10}(OH)_{10}(H_2O)_5]\cdot 14H_2O$ (2301.7): calcd. H 2.28, K 5.10, Mo 41.68, N 0.20, Na 0.70, S 16.72; found H 2.36, K 5.33, Mo 41.16, N 0.24, Na 0.51, S 16.34. EDX atomic ratio found (calcd.): S/Mo = 1.29 (1.20). For this compound, the EDX studies reveal a constant ratio between S and Mo in the analyzed sample, in agreement with the expected formula $[(SO_4)_2Mo_{10}O_{10}S_{10}(OH)_{10}(H_2O)_5]^{4-}$, but suggest also an heterogeneous mixture of salts between Na^+, K^+, and NMe_4^+ cations, the main counterion being in all cases the potassium.

$Rb_{1.4}(NMe_4)_{0.6}[(C_2H_5SO_3)_2Mo_{10}O_{10}S_{10}(OH)_{10}(H_2O)_5]\cdot 8H_2O$ (2): To a suspension of the precursor $K_{2-x}(NMe_4)_x[I_2Mo_{10}O_{10}S_{10}(OH)_{10}(H_2O)_5]\cdot 20H_2O$ (1 g, ca. 0.42 mmol) in water (20 mL) was added ethylsulfonic acid (330 μL, 4 mmol). The pH fell to 1.2. After a few minutes and whilst stirring the pH of the resulting orange suspension was adjusted to 4 with NaOH (4 M), and the mixture was heated at 50 °C for 10 min. RbCl (200 mg, 1.65 mmol) was then added, and the resulting mixture was centrifuged to remove a small amount of a yellow precipitate before it was left to in air. After a few days, hexagonal red-orange crystals were obtained, which were isolated by filtration, washed with cold water, and dried in air (220 mg, 24%). IR (KBr): $\tilde{\nu}$ = 1481 (m, NMe_4^+), 1247 (w), 1156 (s), 1045 (m), 967 (s), 931 (s), 511 (s) cm^{-1}. $Rb_{1.4}(NMe_4)_{0.6}[(C_2H_5SO_3)_2Mo_{10}O_{10}S_{10}(OH)_{10}(H_2O)_5]\cdot 8H_2O$ (2230.8): calcd. C 3.45, H 2.41, Mo 43.08, N 0.38, Rb 5.37, S 17.28; found C 3.42, H 2.38, Mo 42.80, N 0.51, Rb 5.48, S 16.64. ^1H NMR (D_2O): δ = 1.16 (t, J = 9 Hz, 6 H, Me in $EtSO_3^-$), 2.79 (q, J = 9 Hz, 4 H, -CH_2- in $EtSO_3^-$), 3.07 {s, NMe_4^+, ca. 6 H, in agreement with the formula $Rb_{1.4}(NMe_4)_{0.6}[(C_2H_5SO_3)_2Mo_{10}O_{10}S_{10}(OH)_{10}(H_2O)_5].8H_2O$} ppm. EDX atomic ratio found (calcd.): S/Mo = 1.24 (1.2). The ratios involving Rb^+ cation vary as a function of the analyzed crystal suggesting a general formula $Rb_{2-x}(NMe_4)_x[(EtSO_3)_2Mo_{10}O_{10}S_{10}(OH)_{10}(H_2O)_5]\cdot nH_2O$ ($0 < x < 2$).

Preparation of Resins: Synthetic Dowex 50WX2 in acidic form was obtained from Aldrich chemicals. The Dowex-WX2 resins were washed twice with distilled water to remove the excess amount of acid before exchange by Na^+ through suspension of the resins in saturated NaCl solution. After washing by water, the resulting resin was dried at 378 K for 24 h (weight loss of ca 50%) and checked by EDX in order to control its sodium form.

Acknowledgments

This work was supported by the CNRS (UMR 8180) and the University of Versailles. S.F. and J.-F.L. are grateful to Sylvain Cunières for his contribution to the experimental work and to Sophie Chambon for EDX measurements.

[1] M. Bonchio, M. Carraro, A. Sartorel, G. Scorrano, U. Kortz, *J. Mol. Catal. A* **2006**, *251*, 93–99.
[2] A. Sartorel, M. Carraro, G. Scorrano, R. De Zorzi, S. Geremia, N. D. McDaniel, S. Bernhard, M. Bonchio, *J. Am. Chem. Soc.* **2008**, *130*, 5006–5007.
[3] K. Kamata, S. Yamaguchi, M. Kotani, K. Yamaguchi, N. Mizuno, *Angew. Chem. Int. Ed.* **2008**, *47*, 2407–2410.
[4] A. Proust, R. Thouvenot, P. Gouzerh, *Chem. Commun.* **2008**, 1837–1852.
[5] Y. V. Geletii, B. Botar, P. Koegerler, D. A. Hillesheim, D. G. Musaev, C. L. Hill, *Angew. Chem. Int. Ed.* **2008**, *47*, 3896–3899.
[6] A. Ogata, H. Yanagie, E. Ishikawa, Y. Morishita, S. Mitsui, A. Yamashita, K. Hasumi, S. Takamoto, T. Yamase, M. Eriguchi, *Br. J. Cancer* **2008**, *98*, 399–409.
[7] H. Yanagie, A. Ogata, S. Mitsui, T. Hisa, T. Yamase, M. Eriguchi, *Biomed. Pharmacother.* **2006**, *60*, 349–352.
[8] L. Lisnard, P. Mialane, A. Dolbecq, J. Marrot, J. M. Clemente-Juan, E. Coronado, B. Keita, P. de Oliveira, L. Nadjo, F. Sécheresse, *Chem. Eur. J.* **2007**, *13*, 3525–3536.
[9] P. Mialane, A. Dolbecq, F. Sécheresse, *Chem. Commun.* **2006**, 3477–3485.
[10] S. S. Mal, M. H. Dickman, U. Kortz, A. M. Todea, A. Merca, H. Bogge, T. Glaser, A. Müller, S. Nellutla, N. Kaur, J. van Tol, N. S. Dalal, B. Keita, L. Nadjo, *Chem. Eur. J.* **2008**, *14*, 1186–1195.
[11] B. S. Bassil, S. S. Mal, M. H. Dickman, U. Kortz, H. Oelrich, L. Walder, *J. Am. Chem. Soc.* **2008**, *130*, 6696.
[12] Y. F. Song, N. McMillan, D. L. Long, J. Thiel, Y. L. Ding, H. S. Chen, N. Gadegaard, L. Cronin, *Chem. Eur. J.* **2008**, *14*, 2349–2354.
[13] S. G. Mitchell, C. Ritchie, D. L. Long, L. Cronin, *Dalton Trans.* **2008**, 1415–1417.
[14] C. Ritchie, E. M. Burkholder, D. L. Long, D. Adam, P. Kogerler, L. Cronin, *Chem. Commun.* **2007**, 468–470.
[15] E. Cadot, F. Sécheresse, *Chem. Commun.* **2002**, 2189–2197.
[16] E. Cadot, M. J. Pouet, C. R. Robert-Labarre, C. du Peloux, J. Marrot, F. Sécheresse, *J. Am. Chem. Soc.* **2004**, *126*, 9127–9134.
[17] E. Cadot, A. Dolbecq, B. Salignac, F. Sécheresse, *Chem. Eur. J.* **1999**, *5*, 2396–2403.
[18] A. Dolbecq, E. Cadot, F. Sécheresse, *Chem. Commun.* **1998**, 2293–2294.
[19] J. F. Lemonnier, A. Kachmar, S. Floquet, J. Marrot, M. M. Rohmer, M. Bénard, E. Cadot, *Dalton Trans.* **2008**, 4565–4574.
[20] J.-F. Lemonnier, S. Floquet, J. Marrot, E. Terazzi, C. Piguet, P. Lesot, A. Pinto, E. Cadot, *Chem. Eur. J.* **2007**, *13*, 3548–3557.
[21] J.-F. Lemonnier, S. Floquet, A. Kachmar, M.-M. Rohmer, M. Bénard, J. Marrot, E. Terazzi, C. Piguet, E. Cadot, *Dalton Trans.* **2007**, 3043–3054.
[22] E. Cadot, J. Marrot, F. Sécheresse, *Angew. Chem. Int. Ed.* **2001**, *40*, 774–777.
[23] B. Salignac, S. Riedel, A. Dolbecq, F. Sécheresse, E. Cadot, *J. Am. Chem. Soc.* **2000**, *122*, 10381–10389.
[24] E. Cadot, A. Dolbecq, B. Salignac, F. Sécheresse, *J. Phys. Chem. Solids* **2001**, *62*, 1533–1543.
[25] E. Cadot, B. Salignac, J. Marrot, A. Dolbecq, F. Sécheresse, *Chem. Commun.* **2000**, 261–262.
[26] E. Cadot, B. Salignac, S. Halut, F. Sécheresse, *Angew. Chem. Int. Ed.* **1998**, *37*, 611–612.
[27] J.-F. Lemonnier, S. Floquet, J. Marrot, A. Kachmar, M. Bénard, M.-M. Rohmer, M. Haouas, F. Taulelle, M. Henry, E. Cadot, *Inorg. Chem.* **2007**, *46*, 9516–9518.
[28] H. N. Miras, J. D. Woollins, A. M. Slawin, R. Raptis, P. Baran, T. A. Kabanos, *Dalton Trans.* **2003**, 3668–3670.
[29] J.-F. Lemonnier, S. Floquet, J. Marrot, E. Cadot, *J. Cluster Sci.* **2006**, *17*, 267–282.
[30] E. Pehlivan, T. Altun, *J. Hazard. Mater.* **2006**, *134*, 149–156.

[31] In water, at pH 3.5, the spectrum of $K_2[I_2Mo_{10}O_{10}S_{10}(OH)_{10}(H_2O)_5]$ displays two maxima at 281 (ε = 36100 L mol^{-1} cm^{-1}) and 350 nm (ε = 8000 L mol^{-1} cm^{-1}), corresponding to E→Mo charge transfers (LMCT) with E = S or O, in agreement with previous molybdenum wheels in which all the Mo atoms atom exhibit octahedral environment. The spectrum of $K_4[(SO_4)_2Mo_{10}O_{10}S_{10}(OH)_{10}(H_2O)_5]$ under the same conditions exhibits very similar absorption bands with a slight variation in the absorption coefficients, as it increases to 40600 L mol^{-1} cm^{-1} at 281 nm and to 9000 L mol^{-1} cm^{-1} at 350 nm. In the present study, the absorbance of solutions were measured either at 281 nm for low concentrations or at 350 nm for higher concentrations.

Received: June 30, 2009
Published Online: September 16, 2009

